Journal of the American College of Cardiology
© 2005 by the American College of Cardiology Foundation
Published by Elsevier Inc.

Vol. 45, No. 5, 2005
ISSN 0735-1097/05/$30.00
doi:10.1016/j.jacc.2004.11.044

Echocardiography

The Quantification of Absolute Myocardial Perfusion in Humans by Contrast Echocardiography

Algorithm and Validation

Rolf Vogel, MD, PHD, MSEE,* Andreas Indermühle, MD,* Jessica Reinhardt, MD,* Pascal Meier, MD,* Patrick T. Siegrist, MD,† Mehdi Namdar, MD,† Philipp A. Kaufmann, MD,† Christian Seiler, MD, FACC, FESC*

Bern and Zurich, Switzerland

OBJECTIVES We sought to test whether myocardial blood flow (MBF) can be quantified by myocardial contrast echocardiography (MCE) using a volumetric model of ultrasound contrast agent (UCA) kinetics for the description of refill curves after ultrasound-induced microsphere destruction.

BACKGROUND Absolute myocardial perfusion or MBF ($ml \cdot min^{-1} \cdot g^{-1}$) is the gold standard to assess myocardial blood supply, and so far it could not be obtained by ultrasound.

METHODS The volumetric model yielded $MBF = rBV \cdot \beta / \rho_T$, where ρ_T equals tissue density. The relative myocardial blood volume rBV and its exchange frequency β were derived from UCA refill sequences. Healthy volunteers underwent MCE and positron emission tomography (PET) at rest (group I: n = 15; group II: n = 5) and during adenosine-induced hyperemia (group II). Fifteen patients with coronary artery disease underwent simultaneous MCE and intracoronary Doppler measurements before and during intracoronary adenosine injection.

RESULTS In vitro experiments confirmed the volumetric model and the reliable determination of rBV and β for physiologic flow velocities. In group I, 187 of 240 segments were analyzable by MCE, and a linear relation was found between MCE and PET perfusion data ($y = 0.899x + 0.079$; $r^2 = 0.88$). In group II, resting and hyperemic perfusion data showed good agreement between MCE and PET ($y = 1.011x + 0.124$; $r^2 = 0.92$). In patients, coronary stenosis varied between 0% to 89%, and myocardial perfusion reserve was in good agreement with coronary flow velocity reserve ($y = 0.92x + 0.14$; $r^2 = 0.73$).

CONCLUSIONS The volumetric model of UCA kinetics allows the quantification of MBF in humans using MCE and provides the basis for the noninvasive and quantitative assessment of coronary artery disease. (J Am Coll Cardiol 2005;45:754–62) © 2005 by the American College of Cardiology Foundation

Myocardial blood flow (MBF) ($ml \cdot min^{-1} \cdot g^{-1}$), also referred to as absolute myocardial perfusion, is the gold standard to assess myocardial blood supply. It is defined as the blood flow ($ml \cdot min^{-1}$) into a region relative to its mass (g), and so far, can only be determined by positron emission tomography (PET) in humans.

Since the introduction of ultrasound contrast agents (UCA), it has been unsuccessfully attempted to use myocardial contrast echocardiography (MCE) for the measurement of absolute myocardial perfusion. Currently, MCE obtains UCA refill curves after ultrasound-induced microsphere destruction during UCA infusion, and it has been shown experimentally that the respective video intensity $y(t)$ follows an exponential function:

$$y(t) = A \cdot (1 - e^{-\beta \cdot t}) \quad [1]$$

Myocardial plateau signal intensity A and rate constant of rise β have been interpreted as microvascular cross-sectional area and microsphere velocity, respectively. Wei et al. (1) showed in dogs that β and the product $A \cdot \beta$ are semiquantitative estimates of MBF. Although β values vary with different MCE techniques (2), parameter β can be used to assess perfusion changes given that myocardial blood content variations are negligible. The latter assumption introduces a substantial error into the conventional measurement of myocardial perfusion by MCE, because myocardial blood content as reflected by A may vary within and between myocardial regions, with therapeutic interventions or biologic variables such as age, gender, and cardiovascular risk factors. Therefore, myocardial blood content should be directly determined for the comparison of regional perfusion data. However, for parameter A this is impossible because it strongly depends on UCA concentration, scanner settings, and acoustic tissue properties. Hence, the reliability of the product $A \cdot \beta$ is not given, and this emphasizes the need for a robust quantitative method for assessing myocardial perfusion.

From the *Department of Cardiology, University Hospital, Bern, Switzerland; and the †Department of Nuclear Cardiology, University Hospital, Zurich, Switzerland.
This work was supported by grants from the Swiss National Science Foundation (No. 32-58945.99) and the Swiss Heart Foundation.

Manuscript received July 14, 2004; revised manuscript received October 29, 2004, accepted November 16, 2004.

Abbreviations and Acronyms

CAD = coronary artery disease
CCI = coherent contrast imaging
CFVR = coronary flow velocity reserve
MBD = manual bubble destruction
MBF = myocardial blood flow
MCE = myocardial contrast echocardiography
MPR = myocardial perfusion reserve
PET = positron emission tomography
rBV = relative blood volume
UCA = ultrasound contrast agent

Based on a mathematical volumetric model of UCA refill kinetics, we present an algorithm for the quantification of absolute myocardial perfusion using myocardial and blood pool video intensity measurements (Appendix, section A). Myocardial blood flow can be calculated from the blood volume pool relative to the surrounding myocardial tissue (i.e., relative blood volume [rBV]), the exchange frequency of this blood volume, and tissue density ρ_T:

$$MBF = \frac{rBV \cdot \beta}{\rho_T} = \frac{(A / A_{LV}) \cdot \beta}{\rho_T} \quad [2]$$

According to our model, the blood volume exchange frequency equals β, and the rBV can be estimated quantitatively by the division of myocardial plateau video intensity A and the adjacent left ventricular intensity (A_{LV}). The analysis of nearby regions within the myocardium and the left ventricle is proposed to compensate for regional beam inhomogeneities and contrast shadowing.

Objectives of this study were to verify the volumetric model by controlled in vitro experiments, to validate the algorithm versus PET in healthy volunteers, and to demonstrate its applicability to patients with coronary artery disease (CAD) by the comparison with intracoronary Doppler measurements.

METHODS

In vitro experiments. Myocardial tissue and the left ventricular cavity were modeled by hemodialysis filters (mimicking the microcirculation) and polypropylene tubes (mimicking the macrocirculation; inner diameter 8 mm, wall 1.6 mm, Ismatec, Glattbrugg, Switzerland). Two filters were investigated, filter one: Filtral 20 AN69F (Hospal, Meyzieu, France), inner fiber diameter 240 μm, rBV 0.327; filter two: Hemoflow HF80S (Fresenius Medical Care AG, Bad Homburg, Germany), inner fiber diameter 200 μm, rBV 0.213. Filters and polypropylene tubes were connected in series and, by bending the tube into a U-shape, aligned in parallel with a horizontal displacement of 50 mm. The phantom was mounted in upright position. Physiologic saline and UCA was driven down the tube and up the filter by means of a calibrated peristaltic pump (MCP Standard PRO-280, Ismatec). A damping reservoir serving as Windkessel was inserted between the pump and UCA injection site. A closed circuit was established by removing the microspheres via the transmembranous path of a second hemodialysis filter (Hemoflow HF80S, Fresenius Medical Care AG, Bad Homburg, Germany) downstream the perfusion phantom.

For experiments, the phantom was immersed in tap water. The image plane was 11 cm above the filter inlet. The resulting contrast-containing volume between the site of UCA destruction within the tube and UCA detection within the filter was approximately 61 ml and 52 ml for filters one and two, respectively. These volumes prevented the propagation of the destruction zone from the tube into the filter detection zone during the recording of refill sequences. Filters one (two series with complete replacement of filters and tubes) and two were investigated at flow rates between 30 to 230 ml·min^{-1} and 10 to 200 ml·min^{-1}. The resulting filter flow velocities were 1.1 to 8.1 mm·s^{-1} and 0.4 to 8.6 mm·s^{-1} and covered the physiologic range of the microcirculation (3).

Study population. The study protocol was approved by the ethics committees of the universities of Bern and Zurich. A total of 20 healthy volunteers and 15 patients were enrolled in the study. The volunteers had no history of cardiac or pulmonary disease, hypertension, diabetes mellitus, or smoking. Their lipid profile, hemoglobin level, electrocardiogram, and color Doppler echocardiography was within normal limits. The patients who were scheduled for elective coronary angiography were screened for significant coronary artery stenosis. All participants gave written informed consent to participate in the study.

MCE. DATA ACQUISITION. Constant infusion of FS069 (OPTISON, Amersham Health SA, Oslo, Norway) was used for MCE. For in vitro experiments, FS069 was diluted with physiologic saline (1:9) and infused at a rate of 20 ml·h^{-1}. Human studies were performed with parallel intravenous infusion of FS069 3 to 6 ml at a rate of 10 to 20 ml·h^{-1} and physiologic saline at a rate of 400 ml·h^{-1}.

A Sequoia C256 ultrasound scanner equipped with a 3V2c transducer and coherent contrast imaging (CCI) was used for real-time MCE (Siemens Medical Solutions, Mountain View, California). Settings were as follows: mechanical index for microsphere detection 0.08, mechanical index for microsphere destruction 1.3, dynamic range 60 dB, linear postprocessing, clip length 200 frames with triggered intervals of 50 and 75 ms for in vitro and in vivo studies, respectively. Refill sequences were generated using the manual bubble destruction (MBD) feature of the scanner and captured digitally for offline quantification (DataPro 2.11, Noesis S.A., Courtaboeuf, France). Logarithmic signal compression was removed, and linearized intensity data were expressed in arbitrary units.

DATA ANALYSIS. Figure 1A depicts the placement of regions of interest within the microcirculation-mimicking filter and the macrocirculation-mimicking tube. Filter intensity data were corrected for noncontrast signals arising

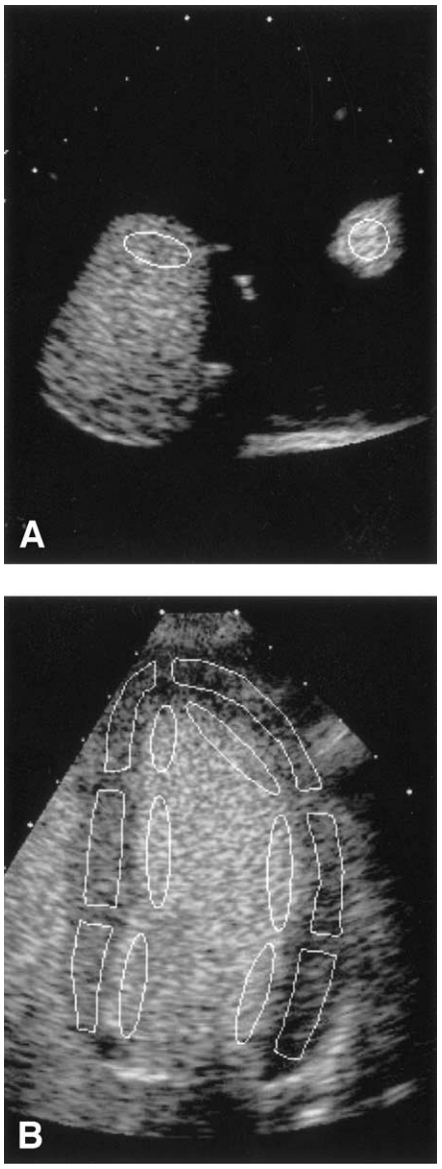

Figure 1. Region-of-interest placement **(solid white lines)** for in vitro and human studies. **(A)** Contrast image of the perfusion phantom, **left** and **right** echo-dense structure represents the cross-section of the hemodialysis filter and the left-ventricular analogue, respectively. The trapezoidal appearance of the filter is caused by total reflectance on the filter housing. **(B)** Four-chamber view of a healthy volunteer.

from filter fibers or trapped air by subtracting the intensity of the first frame after MBD; parameters β and A resulted from fitting to equation (Equation 1). Averaging across the tube lumen yielded A_{LV}; frames during MBD and macrophantom refill were discarded. For the comparison with the independent variable of the perfusion phantom (i.e., pump flow Q_{pump}), absolute filter perfusion assessed by MCE was transformed into total filter flow Q_{MCE} as described in the Appendix, section B.

In vivo, quantitative perfusion analysis was performed on end-systolic frames selected from the perfusion sequence. According to the standard 16-segment myocardial region model, regions-of-interest were placed and tracked manually within the myocardium and in the adjacent left ventricular cavity (Fig. 1B). Myocardial intensity data were corrected for noncontrast signals arising from the tissue by subtracting the signal intensity of the first frame after MBD. Myocardial plateau signal intensity A was calculated using the frames before MBD. Parameter β (s^{-1}) was derived from the frames after MBD. For further analysis β data were transformed into min^{-1}. Signal averaging of all but the frames during and the first one after MBD yielded the signal intensity of the left ventricle A_{LV}. In accordance with PET, ρ_T was set to 1.05 $g \cdot ml^{-1}$, and MBF_{MCE} was calculated with equation (Eq 2). Myocardial perfusion reserve (MPR) was calculated by dividing hyperemic and resting myocardial perfusion.

PET. Positron emission tomography studies were performed using a whole-body scanner (GE Advance PET-Scanner, General Electric, Milwaukee, Wisconsin). An intravenous bolus of ^{13}N-ammonia 700 to 900 MBq was injected for perfusion image acquisition, which was followed by a transmission scan for photon attenuation correction. ^{13}N-ammonia, like UCA in conjunction with the volumetric model, allows the measurement of MBF per total tissue volume (4). Semiautomatic offline analysis (pmod package, PMOD Technologies, Adliswil, Switzerland) yielded MBF_{PET} that was corrected for partial volume effect and spillover.

Cardiac catheterization and intracoronary Doppler study. Patients underwent biplane coronary angiography followed by left ventricular angiography. Intracoronary flow velocity measurements (5) were performed with the 0.014″ JOMETRICS FloWire XT (JOMED, Rancho Cordova, Texas). The coronary flow velocity reserve (CFVR) distal to the stenosis was determined by dividing hyperemic average peak velocity ($cm \cdot s^{-1}$) by resting average peak velocity. Stenosis severity expressed as percent diameter reduction was assessed offline using the catheterization laboratory quantification software (Philips DA, Best, the Netherlands).

Human study protocol. Myocardial contrast echocardiography and invasive studies were performed at the University Hospital of Bern; PET studies were carried out at the PET Center of the University Hospital Zurich. Myocardial contrast echocardiography, PET, and Doppler studies were analyzed by three independent examiners blinded to the other methods' results.

Volunteers of group I (n = 15) and group II (n = 5) underwent MCE and PET perfusion imaging at rest. In group II, MCE and PET imaging was repeated during maximal coronary hyperemia induced by intravenous adenosine 140 $\mu g \cdot kg^{-1} \cdot min^{-1}$.

In patients (n = 15), coronary angiography provided the basis for the selection of the target artery and its myocardial territory. Intracoronary Doppler measurements and MCE were then performed simultaneously at rest and during hyperemia. Hyperemia was induced using an intracoronary bolus of 18 μg adenosine for left and 12 μg adenosine for right coronary arteries. After completion of study-related

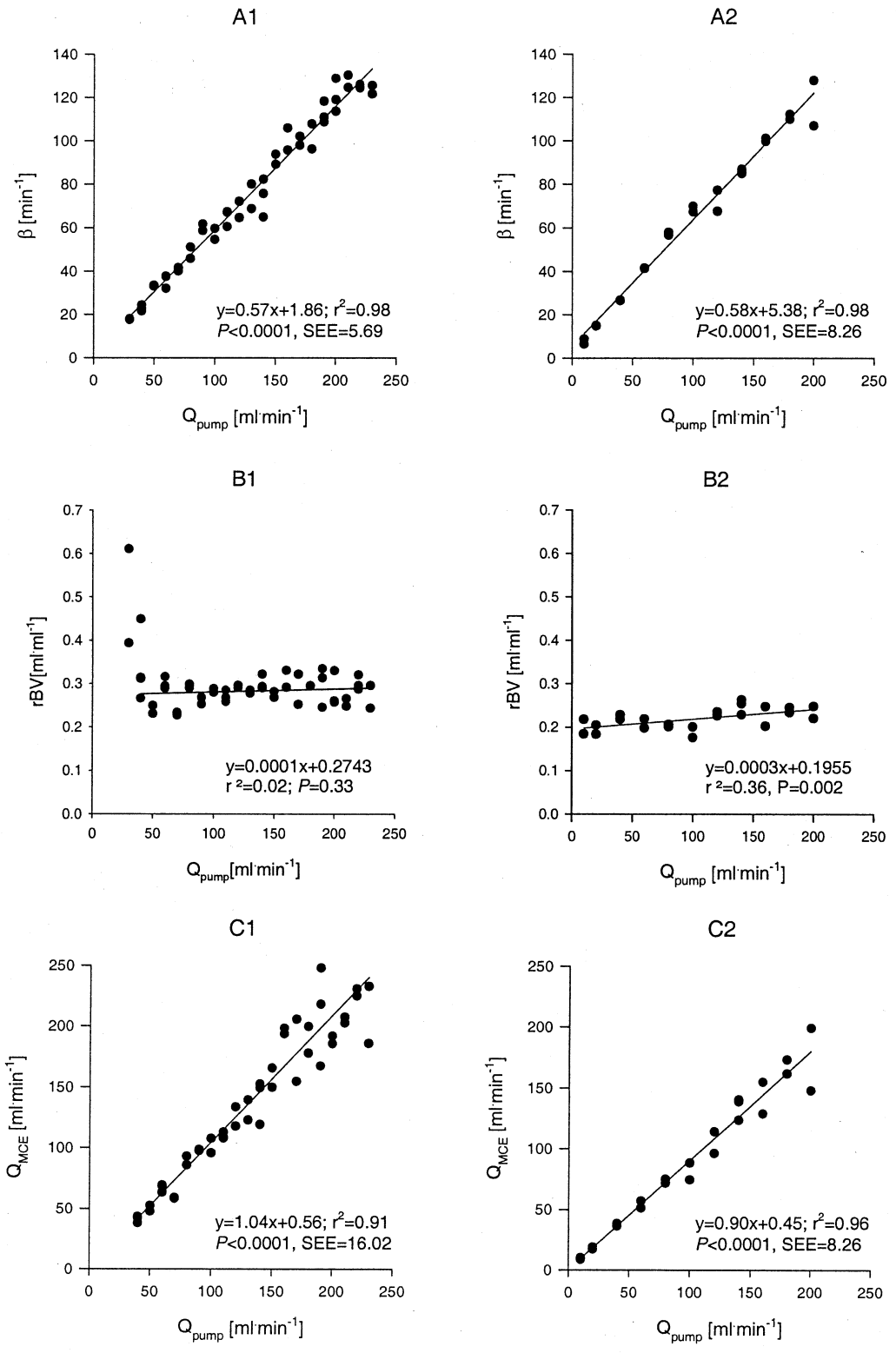

Figure 2. Summary of perfusion studies of filter one **(left panels)** and two **(right panels)**. Myocardial contrast echocardiography (MCE) perfusion parameter β **(A)**, relative blood volume (rBV) **(B)**, and filter flow Q_{MCE} **(C)** are plotted versus calibrated pump flow Q_{pump}. **Solid lines** = regression lines.

Table 1. MCE versus PET: Summary of Hemodynamic and Perfusion Data at Rest (20 Volunteers) and During Hyperemia (5 Volunteers)

Variable	Rest			Hyperemia		
	MCE	PET	p	MCE	PET	p
Heart rate, min^{-1}	66 ± 9	69 ± 11	0.19	91 ± 18	88 ± 19	0.26
SBP, mm Hg	121 ± 13	119 ± 11	0.68	105 ± 10	114 ± 6	0.12
RPP, min^{-1} mm Hg	7,883 ± 1,280	8,252 ± 1,522	0.33	9,645 ± 2,373	10,014 ± 2,159	0.45
MBF, $ml \cdot min^{-1} \cdot g^{-1}$	0.828 ± 0.318	0.826 ± 0.332	0.79	2.801 ± 0.832	2.605 ± 0.781	0.12
β, min^{-1}	8.159 ± 4.811*			19.448 ± 5.512*		
rBV, $ml \cdot ml^{-1}$	0.123 ± 0.045†			0.157 ± 0.045†		

Values are mean ± SD. *$p < 0.0001$; †$p < 0.005$.
MBF = myocardial blood flow; MCE = myocardial contrast echocardiography; PET = positron emission tomography; rBV = relative blood volume; RPP = rate-pressure product; SBP = systolic blood pressure.

measurements, percutaneous intervention was performed where indicated.

Statistical methods. Statistical data are expressed as mean ± SD. Paired and unpaired *t* tests were used for the comparison of dependent and independent samples. Analysis of variance followed by Scheffé's post-hoc testing was used for multiple comparison procedures. Correlations were assessed using linear regression analysis, and accuracy of the prediction was measured by the standard error of the estimate (SEE). Interobserver variability of MCE perfusion data is reported as mean ± SD of differences of paired analysis. Statistical significance was set at $p < 0.05$.

RESULTS

In vitro experiments. Figure 2 summarizes the in vitro perfusion data. As anticipated, measured values of exchange frequency β of filters one and two varied linearly with pump flow. For very low flow rates, the rBV of filter one was overestimated due to insufficient fitting of incompletely recorded slow refill curves, and the data (three measurements) were excluded from the further analysis. Mean ± SD rBVs of filters one and two were 0.284 ± 0.028 $ml \cdot ml^{-1}$ and 0.219 ± 0.023 $ml \cdot ml^{-1}$, respectively. The rBV of filter one was independent of pump flow. In the case of filter two, there was a weak linear relationship between the measured rBV and pump flow (Fig. 2B). For the comparison with the independent variable of the perfusion phantom (i.e., pump flow), absolute filter perfusion assessed by MCE was transformed into filter flow Q_{MCE} (Appendix, section B, equation B 1). Figure 2C shows that MCE provides accurate measurements of pump flow in both filters, the fact which finally corroborates the volumetric model.

Human studies. MCE VERSUS PET. Mean ± SD age of volunteers (3 women, 17 men) was 32 ± 10 years (range 22 to 62 years). Their basic hemodynamic parameters during MCE and PET studies did not differ significantly (Table 1). Figure 3 summarizes the segmental analysis of an MCE perfusion sequence of a 22-year-old female captured from the two-chamber view at rest. Myocardial and left ventricular signals demonstrate regional heterogeneity and are superimposed by cyclic variations with fundamental frequencies between 10 to 12.5 min^{-1}, which are compatible with respiratory movements. In this case, the refill curves did not reach their plateau before clip end, indicating slow exchange of a large blood volume in order to maintain perfusion.

In group I, perfusion analysis by MCE was successful in 187 (77.9%) of 240 investigated segments. Cumulative success rates of inferior, (antero)septal, anterior, and (postero)lateral segments were 93.3%, 92.0%, 66.7%, and 61.3%, respectively. Cumulative success rates of apical, mid-, and basal levels were 91.7%, 81.1%, and 65.6%. Segmental data of β, rBV, MBF_{MCE}, and MBF_{PET} did not differ significantly. Pooling segmental perfusion data revealed the following regional differences. The relative blood volumes of apical (0.108 ± 0.038 $ml \cdot ml^{-1}$) and mid- (0.129 ± 0.049 $ml \cdot ml^{-1}$) levels differed with borderline significance ($p = 0.048$). The rBV of the septal wall (0.135 ± 0.043 $ml \cdot ml^{-1}$) was larger as compared with the lateral wall (0.102 ± 0.040 $ml \cdot ml^{-1}$, $p = 0.01$).

A linear relationship with modest correlation was found between segmental data of β and MBF_{PET} ($y = 6.646x + 2.708$, $r^2 = 0.21$, $p < 0.0001$). Segmental rBVs were normally distributed and correlated weakly with MBF_{PET} ($y = 0.022x + 0.104$, $r^2 = 0.03$, $p < 0.029$). Linear regression analysis and Bland-Altman plot demonstrate good agreement between MBF_{MCE} and MBF_{PET} (Fig. 4); mean ± SD of the measurement difference ($MBF_{PET} - MBF_{MCE}$) was 0.005 ± 0.118 $ml \cdot min^{-1} \cdot g^{-1}$. The interobserver variability assessed in four participants was 0.007 ± 0.120 $ml \cdot min^{-1} \cdot g^{-1}$; segmental success rates of observer one and two were 92.2% and 85.9%, respectively.

In all volunteers of group II, resting and hyperemic perfusion of septal, lateral, and inferior walls, representing the main coronary artery territories, was successfully analyzed by MCE. Figure 5 summarizes MCE and PET perfusion data that demonstrate substantial heterogeneity at rest as well as during hyperemia; MCE and PET measurements of resting and hyperemic MBF were in good agreement. Accordingly, MCE provided accurate estimates of the MPR as determined by PET ($y = 0.89x + 0.21$; $r^2 = 0.81$, $p < 0.0001$, SEE = 0.392).

MCE versus intracoronary Doppler. In the CAD patient group (8 female, 7 male), 18 coronary arteries and their

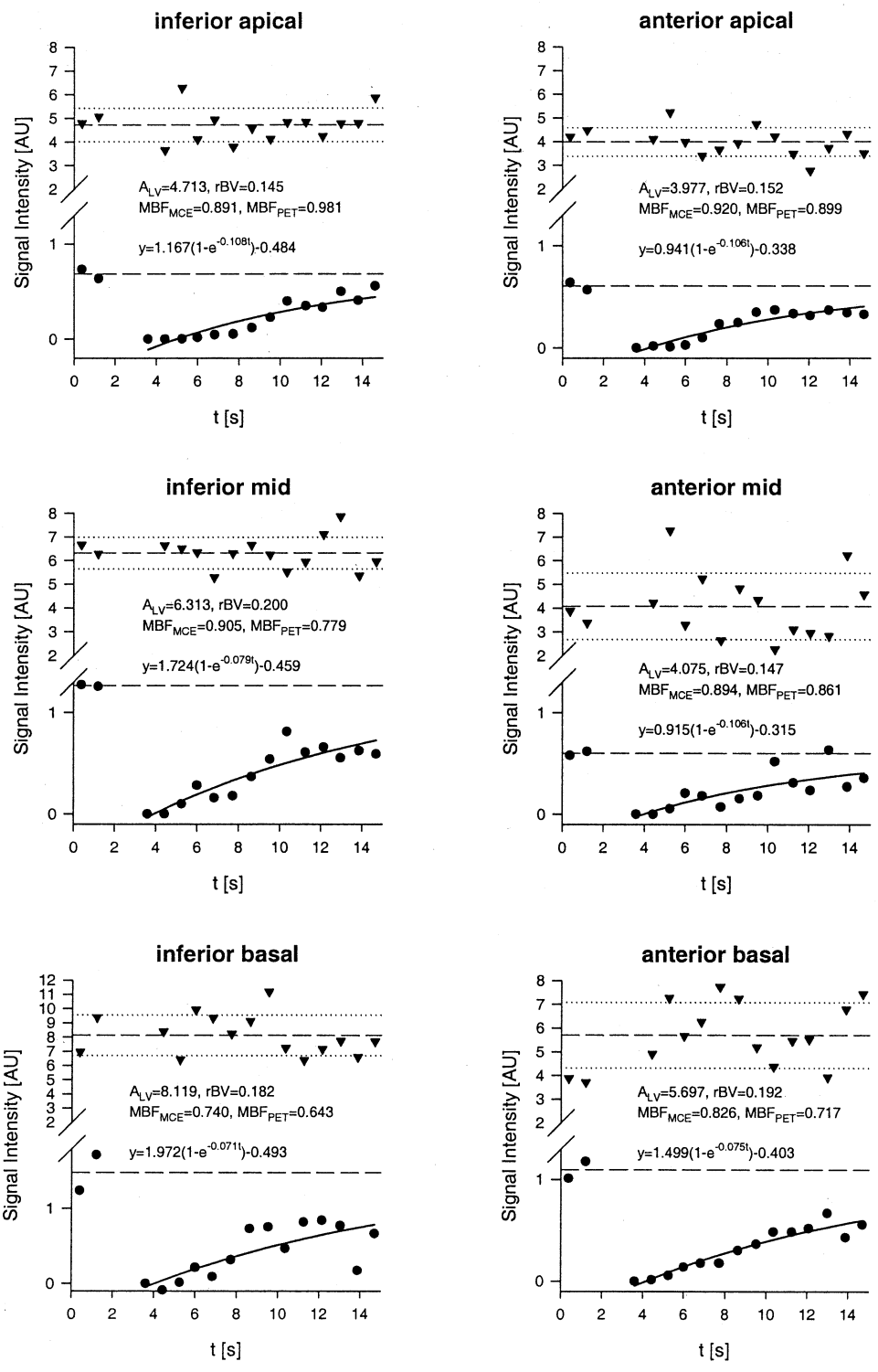

Figure 3. Segmental refill curves **(solid circles)** and corresponding left ventricular signal intensities **(solid triangles)** reconstructed from a myocardial contrast echocardiography (MCE) perfusion sequence at rest. **Upper and lower dashed lines** = A_{LV} and A; **dotted lines** = ± 1 SD of A_{LV}; **solid lines** = the fitting to $y(t) = a \cdot (1 - e^{-\beta \cdot t}) + c$ with the myocardial plateau intensity $A = a + c$. Segmental data of β, relative blood volume (rBV), and myocardial blood flow (MBF) are given in s^{-1}, $ml \cdot ml^{-1}$, and $ml \cdot min^{-1} \cdot g^{-1}$, respectively. For the calculation of MBF_{MCE}, β data were transformed into min^{-1}. PET = positron emission tomography.

JACC Vol. 45, No. 5, 2005
March 1, 2005:754–62

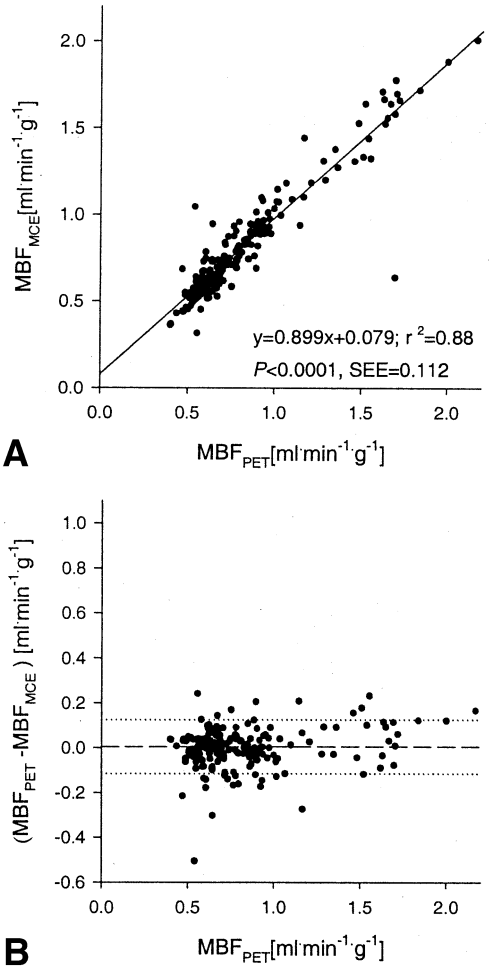

Figure 4. Segmental myocardial blood flow (MBF) data at rest from group I. **(A)** Comparison of myocardial contrast echocardiography (MCE) and positron emission tomography (PET) by linear regression analysis **(solid line)**. **(B)** Bland-Altman plot of MCE and PET perfusion data; **dashed and dotted lines** specify mean ± 1 SD of the measurement difference.

territories were studied (Table 2). Prior myocardial infarction was present in seven patients. The percent diameter reduction of nine coronary arteries was above 50%, while six vessels demonstrated only discrete wall irregularities. In our study population, MPR ($y = -0.02x + 3.13$; $r^2 = 0.45$, $p = 0.02$) and CFVR ($y = -0.02x + 3.17$; $r^2 = 0.50$, $p = 0.001$) decreased linearly with stenosis severity. Figure 6 illustrates the good accordance of coronary vasodilator reserve data measured by MCE and intracoronary Doppler wire.

DISCUSSION

This study, for the first time, presents the theoretical and experimental basis for the quantification of absolute myocardial perfusion or MBF using MCE in conjunction with a volumetric model of UCA refill kinetics and proves the applicability of the algorithm to the human heart.

Myocardial blood flow is determined by the rBV (a measure of vascular density) and its exchange frequency (Appendix, Section B, Equation B 2). Our volumetric

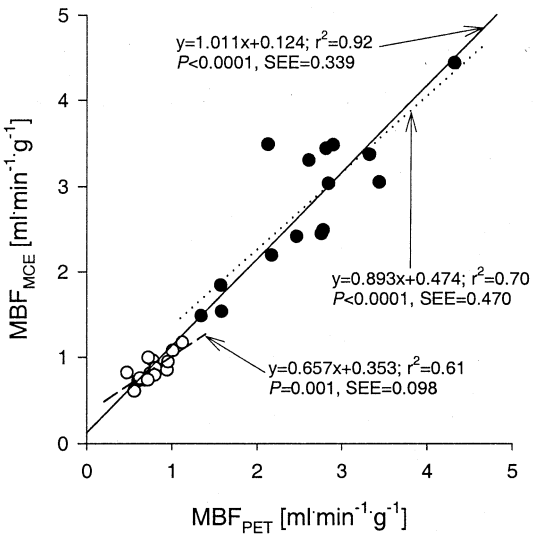

Figure 5. Territorial myocardial contrast echocardiography (MCE) and positron emission tomography (PET) perfusion at rest **(open circles)** and during hyperemia **(solid circles)** of group II volunteers. **Dashed, dotted, and solid lines** indicate regression lines between resting, hyperemic, and pooled perfusion data, respectively. MBF = myocardial blood flow.

model reproduces the experimental refill curve and, therefore, is able to yield the biophysical meaning of parameter β. It is the exchange rate of the blood volume within a myocardial region by means of the blood flow into this region. The comparison of steady state video intensities within the myocardium and a nearby region in the left ventricular cavity yields the rBV. Thus, the assessment of two blood pool intensities in addition to β allows the quantitative measurement of MBF from UCA refill sequences.

In vitro validation. The exact knowledge of rBV is pivotal for determining absolute perfusion. Therefore, tissues with precisely calculable intra- and extravascular compartments such as dialysis filters are required to test the volumetric model. While biologic tissues do not meet this condition

Table 2. Patient Group (n = 15): Patient Characteristics, MCE Perfusion, and Doppler Low Velocity Data

Variable	Mean ± SD or n	Range
Age, yrs	63 ± 13	43–85
Heart rate, min^{-1}	72 ± 10	58–87
Systolic blood pressure, mm Hg	137 ± 27	90–192
Diastolic blood pressure, mm Hg	78 ± 18	57–120
Ejection fraction, %	63 ± 6	50–73
0/1/2/3 vessel disease	5/4/4/2	
Target vessel: LAD/LCx/RCA	9/6/3	
Stenosis, %	40 ± 32	0–86
MBF_{rest}, $ml \cdot min^{-1} \cdot g^{-1}$	0.956 ± 0.281*	0.437–1.450
MBF_{ado}, $ml \cdot min^{-1} \cdot g^{-1}$	2.290 ± 1.090*	0.717–4.309
MPR	2.38 ± 0.89†	1.11–3.74
CFVR	2.44 ± 0.82†	1.1–3.8

*$p < 0.0001$, †$p = 0.62$ (paired t test).

CFVR = coronary flow velocity reserve; LAD = left anterior decending; LCx = left circumflex; MBF_{ado} = hyperemic perfusion; MBF_{rest} = resting perfusion; MPR = myocardial perfusion reserve; RCA = right coronary artery. Other abbreviations as in Table 1.

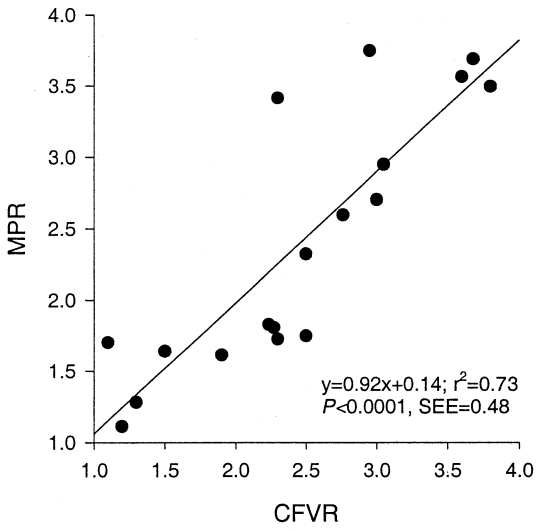

Figure 6. Adenosine-induced coronary vasodilator reserve of the patient group assessed by myocardial contrast echocardiography and intracoronary Doppler velocity measurements. CFVR = coronary flow velocity reserve; MPR = myocardial perfusion reserve.

and standardized phantoms are lacking, the use of hemodialysis filters is the most suitable substitute (6,7). Although being larger than biologic capillaries, filter fibers are still below the resolution of ultrasound and, therefore, fulfill the basic assumption of the volumetric model.

Our phantom meets the simplest design of a cardiac analogue. Sophisticated features such as flow-independent UCA concentration (6) were not implemented for three reasons. First, intravenous UCA infusion is diluted in vivo by the cardiac output similar to our phantom. Second, the algorithm does not rely on absolute microsphere concentrations. Third, any manipulation affecting fiber number or integrity was omitted due to its effects on rBV determination. In our phantom, FS069 microspheres did not adhere to polypropylene tubes or fibers of AN69F and HF80S filters. However, we observed such effects in Nephral (Hospal SA, Meyzieu, France) and Helical (Fresenius Medical Care AG, Bad Homburg, Germany) filters.

Filter flow calculated from MCE perfusion data was in very good agreement with pump flow (Fig. 2C), which proves the correct estimation of parameter β. Furthermore, this indicates system linearity and excludes relevant microsphere destruction during real-time imaging. For filter one, the rBV was underestimated by 13.1%, while the filter flow was measured precisely. This discrepancy most probably can be explained by an overestimation of w_{CCI} (Appendix, section B, equation B 1). The underestimation of rBV may be caused by different acoustic properties of filter housings and fibers, insufficient microsphere transfer via the filter inlet, or a nonlinear contrast signal dilution function of the extravascular compartment.

In vivo validation. Myocardial and left ventricular contrast enhancement variations depend on rBV distribution, local UCA concentration, regional microsphere excitation and destruction, as well as ultrasound beam inhomogeneities, and they may interfere with the quantification algorithm. To address these problems, segmental MBF at rest of 15 volunteers (group I) was studied in detail using typical as well as atypical views in order to assess every segment. As shown in Figure 3, segmental MCE and PET perfusion data vary considerably even in healthy subjects (e.g., apical and midinferior rBVs were 0.145 $ml \cdot ml^{-1}$ and 0.200 $ml \cdot ml^{-1}$). These variations may reflect biologic heterogeneity of regional perfusion parameters as well as measurement errors. However, the final evaluation (Fig. 4), which comprises 187 segments, demonstrates by the excellent agreement between MCE and PET data that video intensity measurements of adjacent regions within the myocardium and the left ventricle obviously correct for regional enhancement changes that are not related to real variations of the rBV.

Dynamic MCE performance was studied in healthy volunteers (group II) and patients with CAD using adenosine-induced hyperemia. In contrast with group I, mean resting perfusion of group II was somewhat overestimated by MCE (11.8%, $p = 0.03$), while there was no significant difference between hyperemic perfusion and MPR data. This finding most probably reflects a sampling problem. The patient group was studied invasively and not by PET, because coronary angiography was mandatory for patient selection, and ad-hoc PCI is customarily performed at our institution. Furthermore, perfusion measurements by PET have never been directly validated in humans with CAD. In our study, MCE was compared with a second reference method (5,8) that allowed the simultaneous acquisition of resting and hyperemic data. Our results confirm that absolute perfusion measurements by MCE can be used for the functional assessment of CAD.

Spatial heterogeneity of resting and hyperemic MBF in healthy humans has already been described (9). Likewise, our regional MBF, rBV, and β data varied considerably within (Fig. 3) and between volunteers (Figs. 4 and 5). Myocardial contrast echocardiography provided exact measurements of MBF although only weak correlations were found between PET perfusion data and the parameters that constitute MBF_{MCE} (i.e., rBV and β). These findings emphasize that the local myocardial blood supply is controlled by the proper balance of local blood volume and its exchange frequency.

Published data in the literature on rBV and β are scarce. In our study, rBVs at rest and during hyperemia were 12.3% and 15.7% in volunteers ($p = 0.005$) and 0.124 $ml \cdot ml^{-1}$ and 0.132 $ml \cdot ml^{-1}$ in patients ($p = 0.34$), respectively. These data are consistent with morphological data from humans (10) and mammals (11–13), revealing a range of 0.05 to 0.20 $ml \cdot ml^{-1}$. Even though being a defined perfusion parameter, human data on parameter β vary with different MCE techniques (2,14–16). This fact and the lack of reference methods for the in vivo assessment of rBV and β further stresses the need for in vitro studies, as presented here, to prove that rBV and β represent the true biophysical quantity.

JACC Vol. 45, No. 5, 2005
March 1, 2005:754–62

Methodological comparison of MCE and PET. As PET, our method calculates MBF from blood pool and myocardial time-intensity curves. Both methods estimate blood volume exchange per sample volume ($ml \cdot min^{-1} \cdot ml^{-1}$) by intensity comparison and kinetic modeling. Blood volume exchange per sample mass ($ml \cdot min^{-1} \cdot g^{-1}$) is then gained by division with tissue density. Because imaging methods cannot determine tissue density, an empirical value of 1.05 $g \cdot ml^{-1}$ is used (17).

Myocardial contrast echocardiography features several advantages over PET such as wide availability, small infrastructure, low cost, and lack of radiation exposure. Furthermore, MCE measurements do not depend on cellular metabolism and are not subjected to partial volume effects and spillover. In contrast with PET, MCE study quality depends on acoustic tissue properties, and measurements will not be obtainable in all patients. To date, MCE perfusion analysis is time consuming, and automated online calculation running on the scanner is required for the routine use of the method.

Study limitations. Relative blood volumes of the examined filters did not cover the range of in vivo data, and the reliability of the quantification algorithm is based on theoretical considerations of acoustic properties. Appropriate in vitro studies were not performed because perfusion phantoms with rBVs substantially below 20% were not available.

Microsphere concentration fluctuations within the macrocirculation (e.g., due to MBD) may propagate into the microcirculation and interfere with the quantification algorithm. While this was prevented in vitro by adapting the image plane, it was not studied in vivo and may play a role, most notably in segments with short supply lines.

The quality of CCI images from parasternal short-axis views, where myocardial anisotropy is significant, was not sufficient for quantitative analysis. Additional compensation may be necessary to account for angle-dependent attenuation encountered by the ultrasonic beam on its way to and from the region-of-interest and within the region-of-interest. In short-axis views, signals from nearby regions in the blood pool will not necessarily be adequate to compensate for these anisotropic effects.

This study was designed to validate MCE for the quantification of MBF in humans while the detection of relevant CAD was not considered. The negative linear relationship between MPR and stenosis severity is a consequence of patient selection, which did not cover mild-to-moderate stenosis. Appropriate clinical trials have to be performed in order to define the method's sensitivity and specificity for the diagnosis of relevant CAD.

Conclusions. The quantification of MBF or absolute myocardial perfusion in humans using MCE in conjunction with a volumetric model of UCA kinetics is feasible and accurate. As a potential bedside technique, this method may promote the impact of perfusion measurements for the clinical management of CAD.

Reprint requests and correspondence: Dr. Christian Seiler, Professor and Co-Chairman of Cardiology, University Hospital Bern, CH-3010 Bern, Switzerland. E-mail: christian.seiler.cardio@insel.ch.

REFERENCES

1. Wei K, Jayaweera AR, Firoozan S, et al. Quantification of myocardial blood flow with ultrasound-induced destruction of microbubbles administered as a continuous venous infusion. Circulation 1998;97:473–83.
2. Dawson D, Rinkevich D, Belcik T, et al. Measurement of myocardial blood flow velocity reserve with myocardial contrast echocardiography in patients with suspected coronary artery disease: comparison with quantitative gated technetium 99m sestamibi single photon emission computed tomography. J Am Soc Echocardiogr 2003;16:1171–7.
3. Fung YC. Biodynamics: Circulation. 2nd edition. New York, NY: Springer, 1984.
4. Bol A, Melin JA, Vanoverschelde JL, et al. Direct comparison of [^{13}N] ammonia and [^{15}O]water estimates of perfusion with quantification of regional myocardial blood flow by microspheres. Circulation 1993;87:512–25.
5. Doucette JW, Corl D, Payne HM, et al. Validation of a Doppler guide wire for intravascular measurement of coronary artery flow velocity. Circulation 1992;85:1899–911.
6. Veltmann C, Lohmaier S, Schlosser T, et al. On the design of a capillary flow phantom for the evaluation of ultrasound contrast agents at very low flow velocities. Ultrasound Med Biol 2002;28:625–34.
7. Lafitte S, Masugata H, Peters B, et al. Accuracy and reproducibility of coronary flow rate assessment by real-time contrast echocardiography. In vitro and in vivo studies. J Am Soc Echocardiogr 2001;14:1010–9.
8. Yoshida K, Mullani N, Gould KL. Coronary flow and flow reserve by PET simplified for clinical applications using rubidium-82 or nitrogen-13-ammonia. J Nucl Med 1996;37:1701–12.
9. Chareonthaitawee P, Kaufmann PA, Rimoldi O, Camici PG. Heterogeneity of resting and hyperemic myocardial blood flow in healthy humans. Cardiovasc Res 2001;50:151–61.
10. Rakusan K, Flanagan MF, Geva T, et al. Morphometry of human coronary capillaries during normal growth and the effect of age in left ventricular pressure-overload hypertrophy. Circulation 1992;86:38–46.
11. Weiss HR, Winbury MW. Nitroglycerin and chromonar on small-vessel blood content of the left ventricular walls. Am J Physiol 1974;226:838–43.
12. Kassab GS, Lin DH, Fung YC. Morphometry of pig coronary venous system. Am J Physiol 1994;267:H2100–13.
13. Judd RM, Levy BL. Effects of barium-induced cardiac contraction on large- and small-vessel intramyocardial blood volume. Circ Res 1991;68:217–25.
14. Wei K, Ragosta M, Thorpe J, et al. Noninvasive quantification of coronary blood flow reserve in humans using myocardial contrast echocardiography. Circulation 2001;103:2560–5.
15. Peltier M, Vancraeynest D, Pasquet, A, et al. Assessment of the physiologic signficance of coronary artery disease with dipyridamole real-time myocardial contrast echocardiography. Comparison with technetium-99m sestamibi single-photon emission computed tomography and quantitative coronary angiography. J Am Coll Cardiol 2004;43:257–64.
16. Shimoni S, Frangogiannis NG, Aggeli CJ, et al. Identification of hibernating myocardium with quantitative intravenous myocardial contrast echocardiography: comparison with dobutamine echocardiography and thallium-201 scintigraphy. Circulation 2003;107:538–44.
17. Schäfers KP, Spinks TJ, Camici PD, et al. Absolute quantification of myocardial blood flow with $H_2{}^{15}O$ and 3-dimensional PET: an experimental validation. J Nucl Med 2002;43:1031–40.

APPENDIX

For the appendix including the volumetric model and perfusion phantom, please see the March 1, 2005, issue of *JACC* at www.onlinejacc.org.